Plasmon-induced Purcell effect in InN/In metal-semiconductor nanocomposites

T. V. Shubina,[1] A. A. Toropov,[1] V. N. Jmerik,[1] D. I. Kuritsyn,[2] L. V. Gavrilenko,[2] Z. F. Krasil'nik,[2] T. Araki,[3] Y. Nanishi,[3] B. Gil,[4] A. O. Govorov,[5] and S. V. Ivanov[1]

[1]*Ioffe Physico-Technical Institute, RAS, St. Petersburg 194021, Russia*

[2]*Institute for Physics of Microstructures, RAS, GSP 105, Nizhniy Novgorod 603950, Russia*

[3]*Ritsumeikan University, 1-1-1 Noji-Higashi, Kusatsu, Shiga 525-8577, Japan*

[4]*GES, UMR5650, Université Montpellier 2–CNRS, Montpellier, France*

[5]*Department of Physics and Astronomy, Ohio University, Athens, Ohio 45701, USA*

(Received 16 July 2010; published 12 August 2010)

The Purcell effect, acceleration of a spontaneous emission recombination rate, has been observed in InN/In nanocomposites with buried nanoparticles of metallic In. This effect, associated with localized plasmons, is characterized by the averaged Purcell factor as high as 30–40 in the structures with large enough particles. This high value is indicative of a noticeable contribution from the emitting dipoles polarized normally to the nanoparticle surface in this system. The experimental observation of shortening of the emission lifetimes with increasing the amount of In is supported by calculations performed in a semiclassical approximation.

DOI: 10.1103/PhysRevB.82.073304 PACS number(s): 73.20.Mf, 71.35.−y, 78.60.−b, 81.07.−b

The desire to create nanostructures combining optical activity of a semiconductor and inherent properties of a metal, such as the strength of collective electron oscillations (plasmons) and high electrical conductivity, has stimulated an interest to metal-semiconductor nanocomposites.[1,2] This class of metamaterials includes hybrid nanostructures (quantum dots, nanobelts), constructed from domains of different materials,[3,4] semiconductor structures covered by a metal film[5] or containing metallic nanoparticles (MNPs) at an interface,[6] and, finally, a semiconductor with buried MNPs.[7]

The enhancement of the emission efficiency in these systems is based on the Purcell effect, i.e., on the increase in spontaneous emission probability of radiating oscillators when they are inserted into a resonant cavity.[8] This effect associated with formation of a coupled state was first considered for metallic particles mixed with a nuclear magnetic medium. The nanocomposite comprising MNPs inside an optically active semiconductor is an analog of such a classical system.

The distinctive of such nanocomposites is that the coupled state occupies a certain volume around a nanoparticle, comprising many dipoles (electron-hole pairs, excitons), which are inevitably differently distant and oriented. It is commonly recognized that the emission efficiency depends on the distance from the MNP and its size.[9–12] Less attention is paid to the fact confirmed recently by site-selective spectroscopy[11] that the strongest enhancement corresponds to the dipole oriented normally to the MNP surface. This phenomenon owes to the parallel (antiparallel) orientation of the "image dipole" with respect to the normal (tangential) orientation of the source dipole.[10,12] The use of the nanocomposites with the buried MNPs is preferable as compared to the MNPs placed above the surface of a semiconductor film since in the latter case the light detected in a conventional backscattering geometry emerges mainly from the emitting dipoles polarized tangentially to the MNP surface.

The confirmation of the Purcell effect implies the direct measurements of the emission lifetimes. Other approaches such as the analysis of emission enhancement must be considered only as supporting. The accelerated dynamics has been previously observed by time-resolved photoluminescence (PL) spectroscopy in several metal-semiconductor structures,[5,6,11,13,14] but not in the nanocomposites with buried MNPs, although the emission enhancement near MNPs in InN epilayers[7,15] was suggestive of this effect.

In this Brief Report, we report explicit evidences of the Purcell effect in the mixed metal-semiconductor nanocomposites, namely, the accelerated radiative recombination dynamics. This effect cannot be ascribed to nonradiative recombination because it is accompanied by the enhancement of an emission intensity. The estimated high value of the Purcell factor (30–40) confirms the importance of the nanoparticles confined within the semiconductor, as well as of the realization of proper particle sizes.

The studies are performed using an InN/In system, in view of the fact that In is a good plasmonic metal for the near infrared range, where optical transitions in InN take place. To form the nanocomposites, pure In insertions separated by 25-nm-thick InN layers were deposited by plasma-assisted molecular-beam epitaxy atop of sapphire (0001) covered by a GaN buffer. The growth runs (performed at the Ioffe Institute) were controlled *in situ* by measuring the laser beam reflection (Fig. 1). The mobility of the In adatoms increases with temperature that promotes their accumulation near defects with the formation of MNPs of large sizes. As a result, the higher is the growth temperature, T_s, the rougher is the sample surface, and the lower is the reflected light intensity.

We focus on the comparative studies of three samples (A, B, and C) with different In amount grown at the same $T_s = 480\,^{\circ}\mathrm{C}$. The sample A consists of six insertions, 48 ML each, which are transformed into large agglomerations of MNPs. In the sample B (20 inclusions of 8 ML), the amount of inserted metal is fourfold less; both size and density of the MNPs are decreased. The average (effective) MNP size varies from hundred nanometer (sample A) to tens of nanometer (sample B). Sample C does not contain such insertions, however, it accommodates spontaneously formed ultrasmall In particles (5–20 nm), revealed by high-resolution transmission electron microscopy.[16] The structures without MNPs,

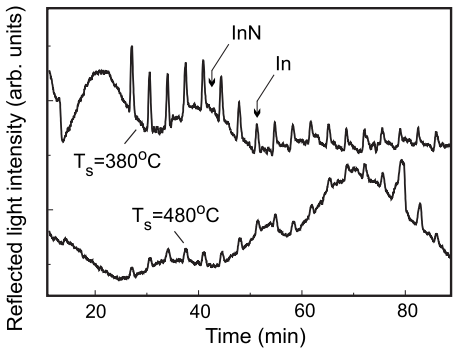

FIG. 1. Variation in the reflected laser light intensity (λ=532 nm) during the growth runs of two samples with similar 8 MLs thick In insertions grown at different temperatures (the scans are vertically offset for clarity).

whose formation can be suppressed, e.g., by using the flux ratio N/In>1, are not considered here because they exhibit much weaker emission.

Figure 2 presents the combined scanning electron microscopy (SEM) and cathodoluminescence (CL) images to show the strong spatial correlation of the intense emission with the large agglomerations of the MNPs. The emission pattern recorded in the structures with small particles is almost uniform. The "spot" registration mode exhibits the CL intensity enhancement up to 65 at the MNP agglomerations. Another intricate feature is certain difference in the emission energy, observed for two closely situated spots, namely, at the dense MNPs agglomeration and apart from it, where the MNPs are separated [Figs. 2(c) and 2(d)]. This can be associated with

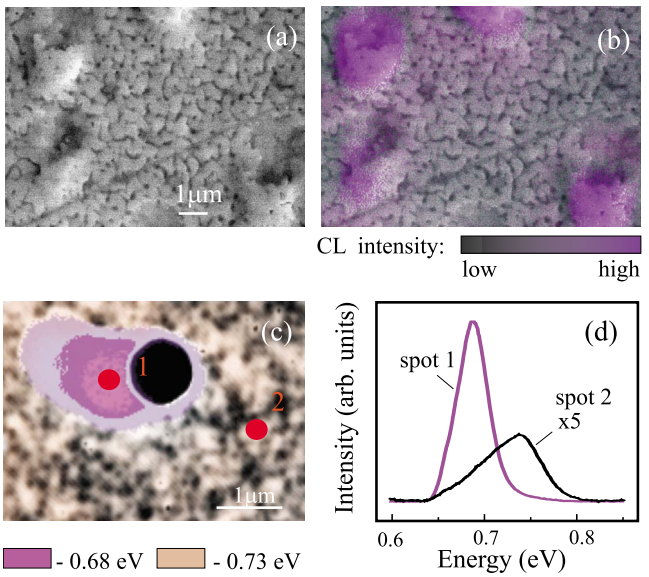

FIG. 2. (Color online) Spatial correlation of infrared emission with In agglomerations in the sample A: (a) SEM image where the agglomerations are visible as lighter areas and (b) combined SEM and mono-CL (0.69 eV) images. [(c) and (d)] Different emission energies in close spots: (c) superimposed SEM and two mono-CL images taken in a sample around an In droplet (round black spot) at 0.68 (violet) and 0.73 eV (beige) energies, (d) spectra recorded in the spots 1 and 2 in (c) marked by red circles.

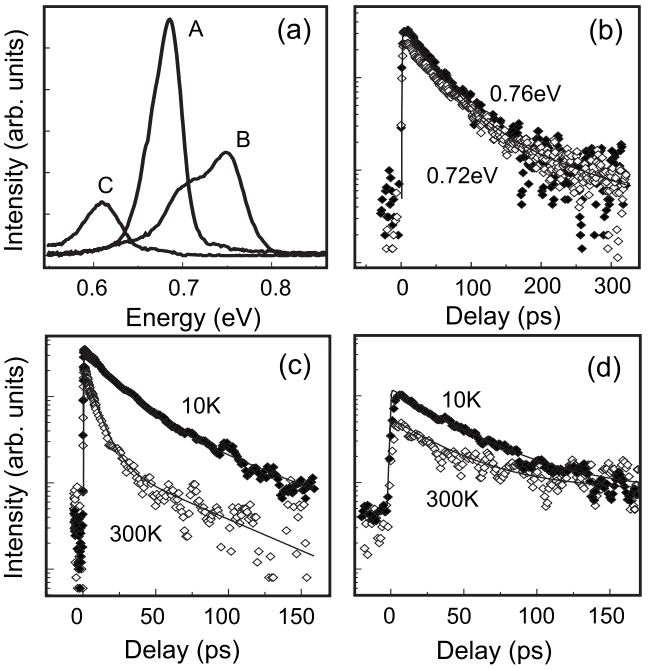

FIG. 3. (a) Low-temperature (20 K) PL spectra measured in three representative samples with the excitation by an 809 nm line of an InGaAs laser diode. (b) PL decay curves (B sample) recorded at different energies: 0.76 and 0.72 eV (τ_1=40 ps and τ_2=200 ps everywhere). PL decay curves recorded in: (c) the A sample at 10 K (τ_1=20 ps and τ_2=70 ps) and 300 K (τ_1=8 ps and τ_2=60 ps) and (d) the C sample at 10 K (τ_1=40 ps and τ_2=1 ns) and 300 K (τ_1=35 ps and τ_2=1 ns).

the collective interaction between the localized plasmons,[17] which lowers the resonance energy by tens of millielectron volt.

In continuous-wave PL spectra [Fig. 3(a)], the difference between the peak energies of the samples A and B, as well as the doublet emission band in the later, is likely induced by this collective effect. The PL intensity is strongest in the sample A in spite of the highest electron concentration $N \sim 10^{19}$ cm^{-3} commonly associated with bad structural quality (in the C sample $N \sim 10^{18}$ cm^{-3}). Thus, there is an apparent tendency for the PL intensity to increase with the creation of the large MNPs.

To reveal the Purcell effect we have used an up-conversion technique which possesses high sensitivity due to the use of visible-range photomultipliers along with high temporal resolution ~150 fs. The measurements exploited FOG-100 (femtosecond optically gated fluorescence kinetic measurement system) combined with a Ti-sapphire laser (Spectra-Physics Tsunami 3960 pumped by Millenia VsJ) emitting light with the quantum energy of 1.55 eV.[18] The luminescence was collected and focused into a nonlinear BBO (beta-BaB_2O_4) crystal. Simultaneously, the light of the delayed exciting beam (probe) was focused on the same spot of the crystal to generate the signal of sum frequency.

The typical PL variation with the probe delay is presented in Figs. 3(b)–3(d). The decay curves are fitted by a sum of two exponents, providing the "fast" and "slow" characteristic PL decay constants (τ_1 and τ_2, respectively). It is commonly

assumed that just the fast component reflects the plasmon-induced acceleration.[5,6,13] In the InN/In nanocomposites, τ_1 turns out to be in the range of 20–50 ps at low temperatures and 8–35 ps at 300 K. The smallest values are registered in the sample A exhibiting the brightest emission. On average, these values are markedly less than the PL decay times reported for pure InN (140–400 ps at PL maxima),[19,20] InGaN/Ag (175 ps),[6] and InGaN/Au (350 ps)[11] structures. The weak acceleration in two latter cases is likely due to the inefficient mutual orientation between the MNPs and the most part of the dipoles.

It is symptomatic that the measured decay constants vary only weakly along the PL spectral contours [Fig. 3(b)] while for such a strongly inhomogeneous semiconductor as InN the noticeable lifetime increase toward the low energy is expected (e.g., from 48 ps to 1.3 ns)[20] due to the carrier localization at various defects. This weak variation in InN/In indicates that some other phenomena, like the Purcell effect, control the PL decay.

Summarizing our experimental findings, we conclude that the accelerated PL dynamics in the structures with large MNPs cannot be ascribed completely to the defect-induced nonradiative recombination because it is accompanied by the enhancement of the PL intensity. The behavior of the structures with small MNPs is contradictive—they do not exhibit such an enhancement, although their PL decay is also quite fast. To clarify this difference, it is worth reminding that the coupled state "MNP—radiating dipole" possesses a fluctuating electrical dipole moment that causes electromagnetic radiation via the radiative channel of the plasmon decay. On the other side, this complex has a powerful channel for dissipative losses—Joule heating due to the nonradiative plasmon decay; for InN/In it was confirmed by the measurements of thermally detected optical absorption.[7,15] To elucidate the dependencies of these two processes on the particle size, we used the semiclassical formalism[10] developed for a metal spheroid with semiaxes a and b. Taking into account only the plasmons polarized along the longest semiaxis a and neglecting the influence of the dipole on the plasmon decay, the radiative Γ_r and nonradiative Γ_{nr} recombination rates in the isolated prolate particle at the resonance frequency ω can be written as

$$\Gamma_r = \frac{4}{9}\left(\frac{\omega f}{c}\right)^3 \frac{\xi}{(\xi^2-1)[Q_1(\xi)]^2}\mathrm{Re}\left[\frac{\partial \varepsilon(\omega)}{\partial \omega}\right]^{-1}, \quad (1)$$

$$\Gamma_{nr} = 2\ \mathrm{Im}\ \varepsilon(\omega)\mathrm{Re}\left[\frac{\partial \varepsilon(\omega)}{\partial \omega}\right]^{-1}. \quad (2)$$

These quantities determine the emission yield $Y(\omega) = \Gamma_r/(\Gamma_r+\Gamma_{nr})$. Here, $Q_1(\xi)$ is a Legendre function of the second kind, $f=|a^2-b^2|^{1/2}$ and $\xi=a/f$. The complex dielectric function of the metal $\varepsilon(\omega)$ is substituted by $\varepsilon(\omega)/\varepsilon_1(\omega)$, when the particle is in a medium with the dielectric function $\varepsilon_1(\omega)$. The plasmon resonance frequency reads as $\omega=\omega_p/[\varepsilon_\infty+\varepsilon_1(L^{-1}-1)]^{1/2}$, where $\omega_p \sim 10$ eV and $\varepsilon_\infty=1$ are the plasma frequency and the background permittivity of the bulk metal. L is the depolarization factor determined by the axes ratio a/b.

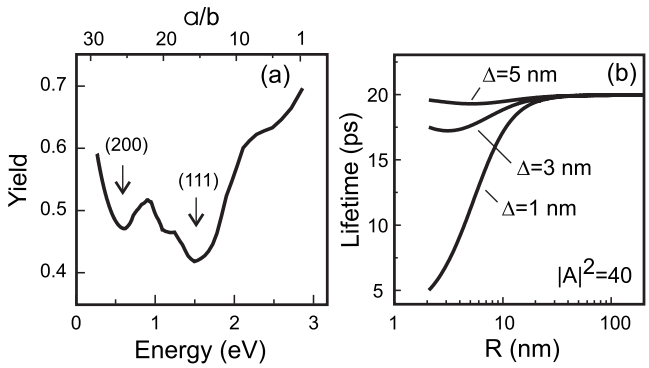

FIG. 4. (a) Dependence of the emission yield Y on the resonant energy determined by an a/b ratio for a prolate particle with the volume equal to that of a sphere with $R=75$ nm. The marked dips are induced by the transitions between parallel bands of In. (b) Combined SEM and mono-CL (0.69 eV) images. The emission spots (violet) coincide with these agglomerations. Emission lifetime versus particle radius calculated for different dipole-particle separation Δ with $|A|^2=40$. The material parameters were taken as for the 0.7 eV energy.

The $Y(\omega)$ dependencies calculated using the experimental dielectric functions of In (Ref. 21) and InN (Ref. 22) are nontrivial [Fig. 4(a)]. The yield drops at 0.6 eV and 1.5 eV due to the (200) and (111) electron transitions between the parallel bands within In, which suppress the plasmonic resonances. At the energy of 0.7 eV, the yield exceeds the 1/2 limit ($\Gamma_r=\Gamma_{nr}$), corresponding to the sizable enhancement, when the volume of the prolate nanoparticle is equal to the volume of a sphere with the radius $R=75$ nm. This radius is somewhat smaller for the oblate and spherical shapes. Overall, the results of the calculations are in line with the observation of the enhanced emission near the large MNPs. It should be noted that the plasmonic resonances are wide and some enhancement exists near 0.7 eV with the MNP shapes statistically distributed around the spherical shape. Thus, the considered spheroid simulates an equivalent action of a distribution of particles of different shapes.

The PL lifetime of a radiating dipole in the presence of an MNP can be, in turn, approximated as

$$\tau_{i,\mathrm{PL}} = \frac{1}{\gamma_r|A_i|^2+\gamma_{nr}+\gamma_{tr,i}}, \quad (3)$$

where i specifies a sample, γ_r and γ_{nr} are the radiative and nonradiative recombination rates of the dipole, respectively, γ_{tr} is the energy-transfer rate from the dipole to MNP. $|A_i|^2$ denotes the Purcell enhancement factor. For the emission process, it equals the square factor of electromagnetic enhancement $|A_i|=|E/E_0|$ determined through the ratio of the local electric field E to the external field E_0. In the dipole approximation, the transfer rate can be written as[23]

$$\gamma_{tr} = \frac{2b}{\hbar}\frac{e^2d^2}{L^6}\frac{3R^3}{|\varepsilon(\omega)+2\varepsilon_1|^2}\mathrm{Im}\ \varepsilon(\omega). \quad (4)$$

Here, d is the interband dipole moment taken as 0.5 nm for InN, $b=2$ is the factor averaging between possible dipole

orientations. $L=R+\Delta$ is the distance between the nanoparticle and dipole centers.

We have calculated the PL lifetimes for various Purcell factors to determine which $|A_i|^2$ values satisfy the measured decay constants. The change in γ_{nr} with the MNP formation was ignored. The values of γ_{nr} and γ_r (100 ps^{-1} and 1 ns^{-1}, respectively) were chosen as corresponding to the average fast and slow PL decay constants recorded in the samples with a negligible amount of MNPs. With these assumptions, the Purcell factor $|A_i|^2=40$ corresponds to the PL lifetime of $\sim$20 ps for the large MNPs [Fig. 4(b)], i.e., to the decay constant recorded in the A sample. The uncertainty in the used parameters implies that $|A_i|^2$ can be between 30 and 40. When the Purcell factor decreases, the prolonged lifetimes are anticipated.

The lifetime shortening with the temperature rise can result from: (i) 1.5-fold increase in Im $\varepsilon(\omega)$ from 4 to 300 K,[21] which in accord with Eq. (2) aggrandizes the critical MNP radius and (ii) delocalization of carriers that stimulates their access to the smallest MNPs, acting as specific nonradiative centers, as well as the contact with the metal surface. Both factors promote the transformation of the electromagnetic energy into heating.[2,12]

The estimation of the Purcell factor based on the fitting of the experimental lifetime gives us an effective value which averages out those corresponding to the optimal conditions (5–8 nm distances, 70–100 nm sizes, and the lined-up dipoles) and those with any deviation from them, suppressing quantum efficiency. More precise calculations must include higher order multipole excitations.[12] It implies also averaging over all possible sizes and distances. It is worth noting that $|A_i|^2\sim 40$ is well consistent with the averaged electromagnetic enhancement factor calculated previously for the statistically dispersed shapes of MNPs and positions of emitters.[7]

The derived Purcell factor is among the highest ever reported for the metal-semiconductor systems.[5,13] We believe that this achievement is mostly provided by noticeable contribution from dipoles oriented normally to the surface of the buried nanoparticles. The reasonably large sizes of MNPs provided by the growth using the periodic In deposition promote the enhancement as well. Resuming, the metal-semiconductor nanocomposites are promising systems to exhibit giant Purcell effect that can be useful for many smart applications.

This work is supported in part by RFBR (Grants No. 10-02-00633a and No. 09-02-01305a) and Presidium of RAS.

[1] E. Ozbay, Science **311**, 189 (2006).
[2] J. R. Lakowicz, Anal. Biochem. **337**, 171 (2005).
[3] R. Costi, G. Cohen, A. Salant, E. Rabani, and U. Banin, Nano Lett. **9**, 2031 (2009).
[4] P. K. Sudeep, K. Takechi, and P. V. Kamat, J. Phys. Chem. C **111**, 488 (2007).
[5] K. Okamoto, I. Niki, A. Scherer, Y. Narukawa, T. Mukai, and Y. Kawakami, Appl. Phys. Lett. **87**, 071102 (2005).
[6] M. K. Kwon, J.-Y. Kim, B.-H. Kim, I.-K. Park, C.-Y. Cho, C. C. Byeon, and S.-J. Park, Adv. Mater. **20**, 1253 (2008).
[7] T. V. Shubina, V. A. Kosobukin, T. A. Komissarova, V. N. Jmerik, A. N. Semenov, B. Ya. Meltser, P. S. Kop'ev, S. V. Ivanov, A. Vasson, J. Leymarie, N. A. Gippius, T. Araki, T. Akagi, and Y. Nanishi, Phys. Rev. B **79**, 153105 (2009).
[8] E. M. Purcell, Phys. Rev. B **69**, 681 (1946).
[9] P. Anger, P. Bharadwaj, and L. Novotny, Phys. Rev. Lett. **96**, 113002 (2006).
[10] J. Gersten and A. Nitzan, J. Chem. Phys. **75**, 1139 (1981).
[11] A. A. Toropov, T. V. Shubina, V. N. Jmerik, S. V. Ivanov, Y. Ogawa, and F. Minami, Phys. Rev. Lett. **103**, 037403 (2009).
[12] H. Mertens, A. F. Koenderink, and A. Polman, Phys. Rev. B **76**, 115123 (2007).
[13] A. Neogi, C.-W. Lee, H. O. Everitt, T. Kuroda, A. Tackeuchi, and E. Yablonovitch, Phys. Rev. B **66**, 153305 (2002).
[14] J. Henson, A. Bhattacharyya, T. D. Moustakas, and R. Paiella, J. Opt. Soc. Am. B **25**, 1328 (2008).
[15] T. V. Shubina, S. V. Ivanov,V. N. Jmerik, D. D. Solnyshkov, V. A. Vekshin, P. S. Kop'ev, A. Vasson, J. Leymarie, A. Kavokin, H. Amano, K. Shimono, A. Kasic, and B. Monemar, Phys. Rev. Lett. **92**, 117407 (2004); **95**, 209901 (2005).
[16] T. P. Bartel, C. Kisielowski, P. Specht, T. V. Shubina, V. N. Jmerik, and S. V. Ivanov, Appl. Phys. Lett. **91**, 101908 (2007).
[17] B. N. J. Persson and A. Liebsch, Phys. Rev. B **28**, 4247 (1983).
[18] V. Ya. Aleshkin, N. V. Vostokov, D. M. Gaponova, V. M. Danil'tsev, A. A. Dubinov, Z. F. Krasil.nik, A. I. Korytin, D. I. Kuritsyn, D. A. Pryakhin, and V. I. Shashkin, Semiconductors **41**, 909 (2007).
[19] R. Intartaglia, B. Maleyre, S. Ruffenach, O. Briot, T. Taliercio, and B. Gil, Appl. Phys. Lett. **86**, 142104 (2005).
[20] F. Chen, A. N. Cartwright, H. Lu, and W. J. Schaff, J. Cryst. Growth **269**, 10 (2004).
[21] A. I. Golovashkin, I. S. Levchenko, G. P. Motulevich, and A. A. Shubin, Zh. Eksp. Teor. Fiz. **51**, 1622 (1963) [Sov. Phys. JETP **24**, 1093 (1967)].
[22] R. Goldhahn, S. Shokhovets, V. Cimalla, L. Spiess, G. Ecke, O. Ambacher, J. Furthmuller, F. Bechstedt, H. Lu, and W. J. Schaff, *GaN and Related Alloys*, MRS Symposia Proceedings No. 743 (Materials Research Society, Pittsburgh, 2003), p. L5.9.1.
[23] A. O. Govorov, J. Lee, and N. A. Kotov, Phys. Rev. B **76**, 125308 (2007).